J Mol Model (2013) 19:289–298
DOI 10.1007/s00894-012-1549-2

ORIGINAL PAPER

Modeling the structure and proton transfer pathways of the mutant His-107-Tyr of human carbonic anhydrase II

Puspita Halder · Srabani Taraphder

Received: 13 June 2012 / Accepted: 23 July 2012 / Published online: 10 August 2012

Abstract We present molecular modeling of the structure and possible proton transfer pathways from the surface of the protein to the zinc-bound water molecule in the active site of the mutant His-107–Tyr of human carbonic anhydrase II (HCAII). No high-resolution structure or crystal structure is available till now for this particular mutant due to its lack of stability at physiological temperature. Our analysis utilizes as starting point a series of structures derived from high-resolution crystal structure of the wild type protein. While many of the structures investigated do not reveal a complete path between the zinc bound water and His-64, several others do indicate the presence of a transient connection even when His-64 is present in its outward conformation. Mutation at the residue 107 also reveals the formation of a new path into the active site. Competing contributions from His-64 sidechain rotation from its outward conformation are also evaluated in terms of optimal path analysis. No indication of a lower catalytic efficiency of the mutant is evident from our results under the condition of thermal stability of the mutant.

Keywords Human carbonic anhydrase · Network analysis · Potential of mean force expansion · Proton transfer · Water reorganization

Introduction

In a proton transfer reaction taking place at or near the active site of an enzyme, an excess proton is assumed to be relayed through the local-area-network or "pathway" of hydrogen-bonded clusters formed by the polar amino acid side chains and water molecules present in a "proton channel" of the protein [1–4]. Starting from a known high-resolution structure of the protein, one may analyze the hydrogen-bonded network present, if any, to identify probable proton-transfer pathways. The pathways thus detected for the wild type protein can be compared to those found in the mutants to evaluate the role of specific residues forming the proton transfer paths [5]. However, only disconnected fragments of network or "path" are NMR studies or trajectories simulated up to a few nanoseconds. These missing connectivities in the proton-conducting network may be formed transiently from the cooperative fluctuations of protein structure and hydration over a broad range of time scales [6]. Therefore, an understanding of the coupling of protein motion and water reorganization to proton transport is crucial in deriving the mechanism of enzyme catalyzed proton transfer reactions.

Carbonic anhydrases (CAs) are zinc-metalloenzymes, which utilize a rate-limiting proton transport (PT) step in their enzymatic reaction [1]. Among several types of CAs found in varieties of organisms such as microbial organisms, plants and animals, HCA II is one of the most efficient enzymes known and it reversibly catalyzes the hydration of CO_2 to HCO_3^- (or vice versa) with a maximal turnover rate of 10^6 s^{-1} at 25°C. HCA II is a cytosolic enzyme consisting of a single polypeptide chain of 260 amino acid residues. The catalytic center of the spherically shaped enzyme resides at the bottom of a conical cleft. At the base of this cleft there exists a Zn^{2+} ion which is tetrahedrally coordinated to three histidines (His-94, His-96 & His-119) and a water/hydroxide ligand [1]. The zinc-bound water molecule is generally referred to as the "zinc-water" and its *pKa* is found to be near 7 [7]. In the most widely accepted hydration mechanism, the first step of catalysis involves nucleophilic attack of zinc-bound hydroxide on CO_2 to produce zinc-bound HCO_3^- which is subsequently replaced by a solvent water molecule [8]. The next two steps involve

P. Halder · S. Taraphder (✉)
Department of Chemistry, Indian Institute of Technology, Kharagpur 721302, India
e-mail: srabani@chem.iitkgp.ernet.in

re-generation of zinc-bound hydroxyl ion by the active participation of proton-shuttling His-64 residue of the protein moving from "inward" to "outward" conformations to maintain the flow of the catalytic cycle. First, an intramolecular proton transfer between zinc-water and inward conformer of His-64 residue constitutes the rate-determining step [9] which seems to be mediated by a chain of few water molecules at the active site. The next step is followed by an intermolecular proton transfer from the "outward" conformation of protonated His-64 to the bulk solvent. This intermolecular proton exchange is found to be rate limiting at low buffer concentrations. Thus His-64 is believed to act as a proton shuttling residue between the active site and solvent exposed surface of the protein during the catalysis although the mechanistic details are still being investigated [10, 11]. In addition to His-64 orientation, the hydrogen bonded clusters primarily comprised of water molecules at the active site have also been shown to form alternative, *albeit* less efficient pathways and these are summarized below [6] and are represented in Fig. 1.

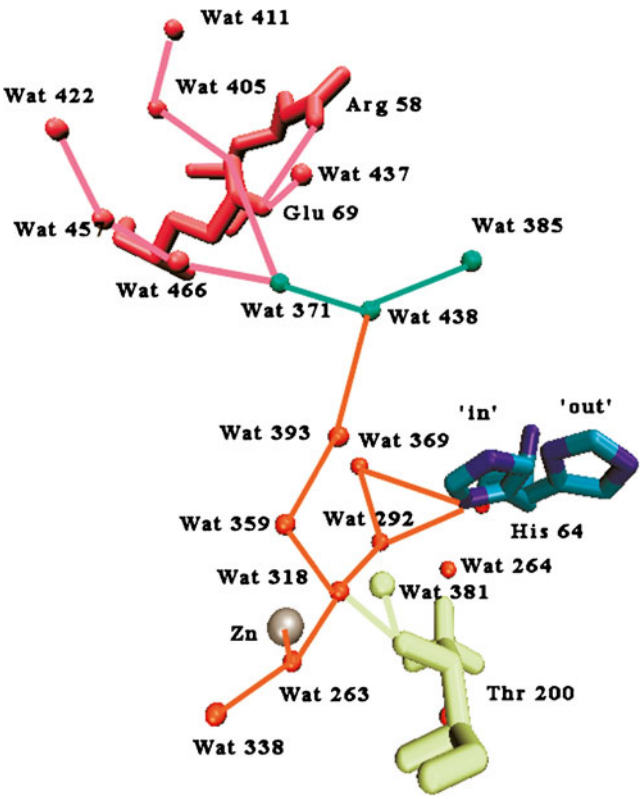

Fig. 1 Representation of proton transfer paths at the active site of the wild type HCA II. The major path is mediated by His-64, shown with its two sidechain conformers with 'in' and 'out' orientations. Active site water molecules facilitate four different alternative paths labeled as Alt-1 (*red*), Alt-2 (*green* and *magenta*), Alt-3 (*yellow*) and Alt-4 (*green*)

- *Path Alt-1* is formed by a small disordering of water molecules near His-64 that directly opens up the active site network cluster to the solvent through Wat-393.
- *Path Alt-2* is formed by the hydrogen-bonded cluster containing Glu-69 and Arg-58 and other water molecules with several nodes of the network exposed to the solvent.
- *Path Alt-3* is a short path mediated by Thr-200 and a few other water molecules.
- *Path Alt-4* is a shorter segment of the path Alt-2 when due to disordering; some water molecules such as Wat-385 may become directly accessible to the bulk solvent.

The residue/water numbers indicated as above are the same as those in the crystal structure (PDB id: 2CBA) [1]. A large number of single and double mutants of HCA II has been shown to exhibit facilitation or suppression of one or more of these pathways that correlate well with their observed activities [12].

In this work, we investigate the effect of His-107-Tyr mutation on the proton transfer path of HCA II. It is well known from the literature that His-107 residue is conserved in all of the carbonic anhydrases sequenced to date [13], except for the class of plant carbonic anhydrases. In spite of its location near the active site region, it does not appear to play a direct role in the catalytic mechanism [14]. However, the possibility of an indirect influence on the enzyme action may not be completely ruled out as replacement of His-107 by Tyr has an immense physiological significance. This mutation has been reported to cause the genetic disease called carbonic anhydrase II deficiency syndrome (CADS). This is also known as marble brain disease (MBD) or Guibaud-Vainsel syndrome in humans comprising renal tubular acidosis, osteopetrosis and in some cases mental retardation [15]. Mutation at the residue 107 has been correlated primarily to the misfolding of the native protein structure which in turn induces structural instability of the mutant protein. Tu et al. reported [16] that this mutant was so unstable that it was very difficult to get the protein in pure form. They were able to stabilize and store it at 4°C only in cell lysates containing 1-4 mg/ml bovine serum albumin (BSA). The specific interaction of the mutant His-107-Tyr of HCA I1 with BSA was assumed to involve the formation of electrostatic and possibly hydrophobic interactions with surface residues. Such interactions of the cellular components were probably the source of stability of the mutant in concentrated cell lysates. From the kinetic studies the catalytic activity of this mutant is found to be three-fold reduced to that of wild type HCA II expressed under similar conditions [16]. The observed loss of activity has been attributed to the significant thermal instability of the enzyme as well as to lower efficiency of the proton transfer pathways compared to the wild type protein [17]. The loss of enzymatic activity is also evident from the midpoint temperature of denaturation which has a value of 22°C for the mutant compared to 61°C for the

wild type protein. Guanidium hydrochloride-denaturation study at 4°C of temperature showed that the native state of the mutant was destabilized by 9.2 kcal mol^{-1} with respect to the wild type protein [18]. Preliminary investigation of model structures [16, 18] of the mutant His-107-Tyr indicated that replacement of the imidazole group of this side chain causes the loss of at least two hydrogen bonds to the side chain of Glu-117, although the interaction of the backbone NH of Tyr to Glu-117 is preserved. While the hydrogen bond between His-107 and Tyr-194 is lost, one new hydrogen bond between the hydroxyl group of Tyr-194 and Ser-29 is detected in the mutant structure [16]. These hydrogen bonding interactions are represented in Fig. 2a for the wild type protein and in Fig. 2b for its mutant. This introduces the possibility that structural variations in residue 107 might influence the geometry, and therefore the reactivity, of the zinc-water complex. In the previous studies with this mutant, His-107 was found to be a part of long hydrogen bonded network that originates from active site Zn^{2+} coordinated ligand, His-119 and ends at Trp-209 with the following sequence of amino acid residues [1] : His-119→Glu-117→His-107→Tyr-194→Ser-29→Ser-197→Trp-209. By disrupting His-107 residue, the above mentioned hydrogen-bonded network also becomes ruptured which might be one of the reasons for its instability and lower activity. In addition, the bulky Tyr residue occupies a much larger volume (204 $Å^3$) compared to His (167 $Å^3$) which may lead to a slight distortion of the active site cavity [16]. The observed reduction in the catalytic activity may thus signify an important role of the thermal stability and active site distortions on the mechanism of function of the mutant.

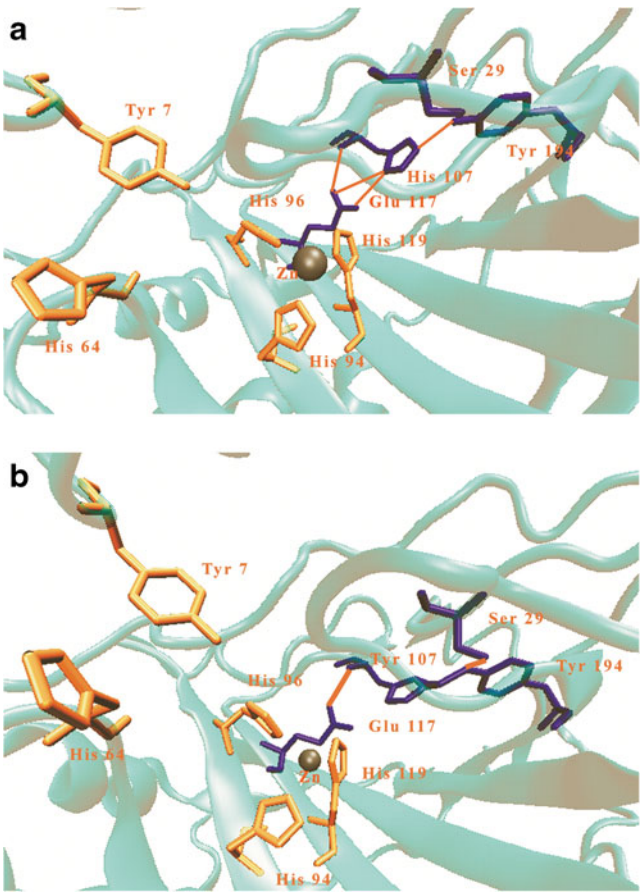

Fig. 2 Important amino acid residues taking part in hydrogen bonding interactions around residue 107 for (**a**) wild type HCA II (crystal structure with pdb id: 2CBA) and (**b**) His-107-Tyr mutant of HCAII (input structure to model 1)

In view of the above discussion, it appears appropriate to pose the following questions. Is it possible to generate an ensemble of thermally stable structures of the mutant below its melting temperature? We emphasize on obtaining the ensemble to be able to carry out a statistically relevant sampling of key structural fluctuations. Do the pathways detected in the wild type enzyme persist in this mutant in the range of temperature where it is thermally stable? Can we correlate, at least qualitatively, the observed changes in catalytic activity of the mutant to the detected pathways? What is the role of Tyr-107 residue forming putative proton conducting pathways of the mutant particularly in the context of structural disruptions mentioned above? In this article, our objective is to investigate these issues by carrying out a detailed detection of possible proton transfer pathways in this particular mutant of HCA II. Since no high resolution structure is available for this mutant till date, we have utilized in our analysis a set of model structures. The first set of structures was obtained from the crystal structure of the wild type protein (pdb id: 2CBA) [1] by *'in silico'* single point mutation of the respective residue. Further refinements of this structure were carried out by introducing disordered water locations in separate models using the method of potential-of-mean-force [19] and molecular dynamics simulations. In each case, potential proton pathways are identified and compared to those observed in the wild type crystal structure. The role of His-64 conformational fluctuations is investigated by carrying out an extensive, conformational space sampling of the protein coupled to probable disordering of interior hydration sites. Our results show that in the mutant His-107-Tyr, the potential proton paths at the active site can be closely mapped onto the four possibilities indicated as Alt-1, 2, 3, and 4 as in the case of the wild type enzyme. Moreover, additional transient connections to the protein surface are detected in the region of mutation. These observations are then correlated to the mechanism of proton transfer in the mutant.

Theoretical methods

Due to the unavailability of any stable crystal structure of the mutant protein, the very first step in our analysis required us to generate a model structure of the mutant. Starting from the crystal structure of wild type HCA II (pdb id

2CBA) [1] as input, we replaced the His-107 residue with Tyr by using the mutation utility of NAMD (molecular dynamics package) [20]. The model structure, thus generated, is assumed to represent the positions of heavy atoms like C, O, N, S and also the three dimensional structure of the protein including backbones and sidechains.

It is widely understood that an accurate model for the hydration sites within the protein matrix is essential for a correct detection of the hydrogen-bonded networks forming putative proton paths. To describe the positions of water molecules within the enzyme, three different models have been used in the present study.

Model 1: All the water positions derived from the crystal structure of the wild type protein have been retained.

Model 2: A series of structures has been generated by including variations in and around the hydration sites of model 1 within the protein, derived by using the potential of mean force method (PMF) [19]. Such variations in the water sites are expected to reflect transient hydration of the active site cavity by water molecules permeating from the surface and/or disordering of highly mobile water molecules about their crystal positions relevant at the time scale of reaction. In the potential of mean force method [19], the probability density of hydration at a given site inside the protein is approximated as the combination of two- and three-particle correlation functions of protein atoms with water. The locations thus identified and having populations above a chosen cutoff are recursively included in our study as probable hydration sites either in addition to the water positions as in model 1 or as approximations of locations to which the active site water molecules may reorganize. In the present work, we have labeled the derived water positions based on the ratio (ρ/ρ_0) of probability densities at a given site to that in bulk water as [19]

- **high density site** ($3.0<\rho/\rho_0<4.0$)
- **low density site** ($2.0<\rho/\rho_0<3.0$)

Model 3: In this model, the water structure has been derived from classical molecular dynamics simulations of aqueous solutions of the His-107-Tyr mutant of HCA II employing NAMD [20]. The model structure generated by mutating the His-107 residue with Tyr is used as input for the simulation. The simulated system contains the monomeric protein consisting of 260 amino acid residues solvated in a large cubic box with around 14,500 TIP3P water molecules using the utilities of NAMD [20] and VMD [21]. Before starting the simulation, we removed all the water molecules that are within 3.8 Å of any protein atom. The CHARMM22 force field [22] and potential parameters were used to compute the pair interactions. Two chloride ions were introduced in the system to maintain overall electroneutrality and to simulate the microscopic environment corresponding to a neutral pH. The protonation states of the amino acid residues were chosen accordingly and a water molecule was attached to the doubly charged zinc ion. We performed the minimization run for 500 ps followed by 1 ns equilibration and 1 ns production runs under isothermal-isobaric (NPT) conditions at 1 atm and 293 K. The simulation temperature is chosen to be somewhat lower than the experimentally known melting temperature of the mutant so that stable solvated structures may be sampled and corresponding fluctuations in water positions recorded. The dynamical equations were solved using the multiple time step algorithm (RESPA) with a MD time step of 2 fs. For electrostatic interactions, we have used the particle-mesh-Ewald (PME) summation method with periodic boundary conditions. The pressure is kept constant at 1 atm utilizing Langevin piston method with a damping co-efficient of 5 ps^{-1} [23] and the temperature is fixed at 293 K through Langevin damping with a co-efficient of 5 ps^{-1}. The list of non-bonded interactions is truncated at 13.5 Å and a switching cut-off distance of 10 Å is used for Lennard-Jones interactions.

All the structures of the mutant generated as described above are subsequently examined to obtain optimized proton transfer paths [6, 24] between the sidechain atoms of His-64 and the hydrogen bonded water cluster at the active site. We report here the results of path analysis when His-64 sidechain is present in its 'outward' orientation. Starting by enlisting the heavy atoms of all polar amino acid residues and O atoms of water molecules as probable nodes in a proton relay, we have classified them in hydrogen-bonded clusters using an upper cutoff of 3.5 Å [24]. A complete path is detected when any of these clusters have sidechain ($N_{\delta 1}$ and $N_{\varepsilon 2}$) atoms of His-64 and node(s) contributed by the active site atom(s) including O of water molecules are solvent-exposed. In the absence of any *complete* path, we next carry out an extensive, Monte Carlo based sampling of the conformational space of the protein with special emphasis on the rotation of His-64 sidechain from its outward to inward orientation. This sampling enables us to detect transient connectivities that may form by fluctuations in sidechains and water positions within the protein and contribute to the completion of proton path across the active site. For each such transient connection detected, the probability of connecting the corresponding nodes is calculated [24]. For this purpose, we model pair interactions using the parameters of CHARMM22 forcefield and set up an $M = \sum_{i=1,n} m_i$ -dimensional energy matrix (with a 5° periodic grid in each

dimension) representing the conformational space of n residues with m_i dihedral angles $(i=1,n)$ each [24]. An optimal path for each transient connection is then obtained by employing Dijkstra's algorithm [25, 26] with the smallest energy cost where energies are expressed in k_BT units. Here k_B represents the Boltzmann constant and T represents the absolute temperature.

Results and discussion

In this section, we present the results of our investigation on probable proton transfer paths in the mutant His-107-Tyr of HCA II and compare them to those obtained in the wild type protein. We first report the role of reorganization of water molecules on the formation of these putative paths in the mutant. The effect of protein motions such as His-64 side-chain fluctuation is also probed and the importance of both the factors evaluated.

Water occupancy and network analysis

Two different regions of the protein have been probed at length; first, the active site and the associated water structure near the key residue His-64; second, the site of mutation and the structure of hydrogen bonded network in its vicinity. In the first case, we investigate the pathway between the zinc water and His-64 and the second one allows us to examine if any additional nodes are provided to the network by changes at the mutation site.

Model 1

In this model, we have used the locations of water molecules at the active site and at the site of mutation as derived from the crystal structure (PDB id: 2CBA) [1] of HCA II. In each case, we have compared these locations with those derived from another high resolution crystal structure (PDB id: 2ILI) [27]. As shown in Figs. 2a and b, both sets of data provide nearly identical representation of the hydration sites corresponding to the pathways of interest.

At the active site of the mutant

In Fig. 3a, we have highlighted the hydration structures at the active site within a radial distance of 12 Å from the catalytic Zn^{2+} ion. Marked differences are noted in the hydration structures from the two sets near the residue Glu-69. In the region intervening the active site water cluster and His-64, it therefore appears reasonable to use the hydration sites as detected in the crystal structure with PDB id 2CBA [1] for the mutant in our network analysis. It may be noted that in both the crystal structures mentioned above,

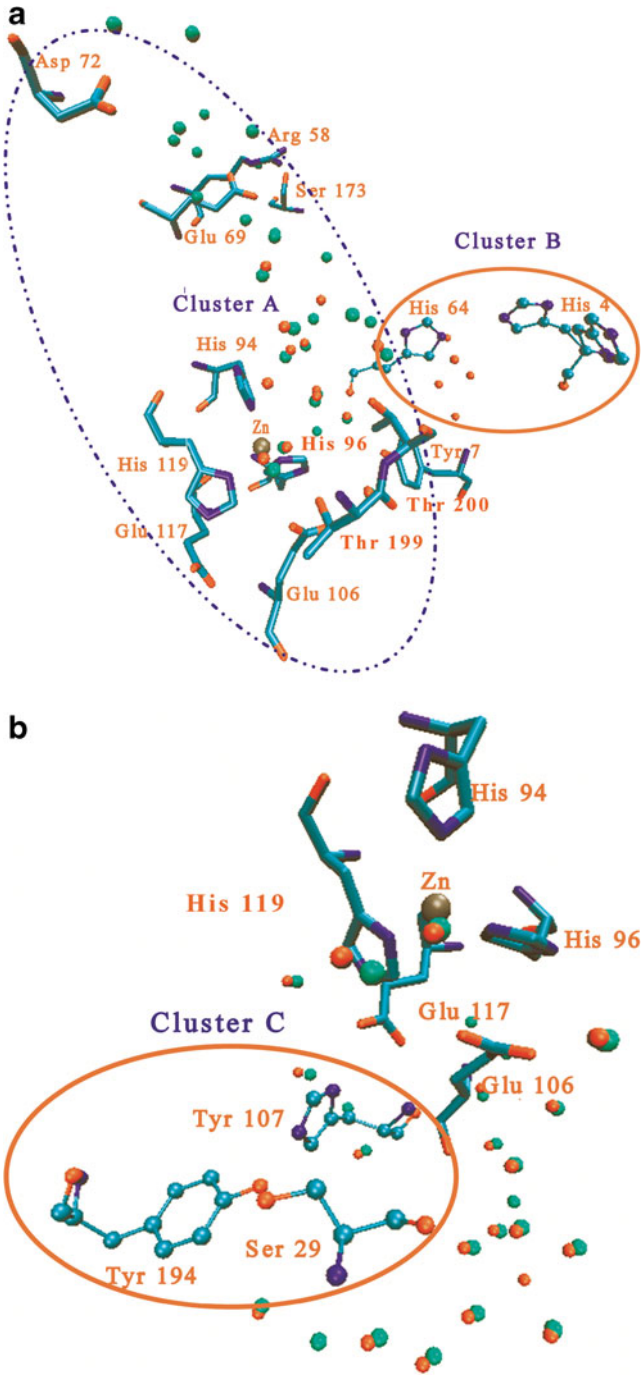

Fig. 3 Comparison of (**a**) active site and (**b**) mutation site hydration structures of wild type HCAII (from crystal structures with pdb id: 2CBA, shown in red and pdb id: 2ILI, shown in green) and the His-107-Tyr mutant of HCA II (same structure as in Fig. 2)

the zinc water belongs to a large hydrogen bonded cluster (labeled as cluster A) at the active site. His-64 in its outward conformation is found to be a part of a much smaller cluster (labeled as cluster B). The crystal structure with PDB id 2CBA [1] reveals cluster A to be buried and cluster B as having solvent exposed nodes. Interestingly, cluster A (in the structure 2ILI) [27] is comprised of solvent exposed

nodes while cluster B remains buried. However, the desired path between the zinc-water and His-64 sidechain could not be detected in either of these wild type structures.

Recursive network analyses of the mutant reveal that as in the wild type structure, clusters A and B can still be detected. However, cluster A in the mutant is comprised of 26 hydrogen-bonded nodes while that of the wild type had 30 network nodes [6]. This difference arises from the fact that the residues Ser-29, Tyr-107 and Tyr-194 are no longer connected to cluster A. They form a new cluster that is completely buried within the protein. This has been represented as cluster C in Fig. 3b. Thus, the above analyses do not indicate any involvement of His 64 in the formation of a path originating from the zinc water in the mutant protein.

Around the mutation site

We have shown in Fig. 3b the locations of water molecules around the site of mutation and within a radial distance of 11 Å from the C_α atom of residue 107 of the mutant. The corresponding water positions as derived from the other crystal structure (PDB id: 2ILI) [27] indicate the suitability of the present model to mimic the hydration structure in the mutation region. The subsequent network analysis shows that cluster C, as mentioned above, appears to be the only potential path in this region, but none of the water molecules shown in Fig. 3b are found to be connected to this cluster. Therefore, within this model, no proton transfer path is detected near the mutation site that leads to a solvent exposed node.

Model 2

At the active site of the mutant

Using the PMF method [19], we have calculated the probability density of hydration by a recursive sampling method spanning a wide region of the active site. First, we choose a cubic region of length 7 Å in each direction with a periodic grid interval of 0.25 Å and centered round the catalytic Zn^{2+} ion. We have subsequently repeated the analysis by placing the center of the sampling box at the crystallographic water positions such as W1 (Wat-318), W2 (Wat-292), W3a (Wat-264) and W3b (Wat-369). All these water sites have been suggested to be directly involved in forming the crucial proton transfer cluster between the zinc-water and His-64 [28]. The numbers shown in parenthesis refer to those used in the X-ray crystallographic structure of wild type HCA II (PDB id: 2CBA) [1]. In Fig. 4a, we have shown the distribution of water sites as obtained from the PMF study along with W1, W2, W3a and W3b. The highlighted locations of high and low density hydration sites (obtained from our calculations) are found to be clustered predominantly at

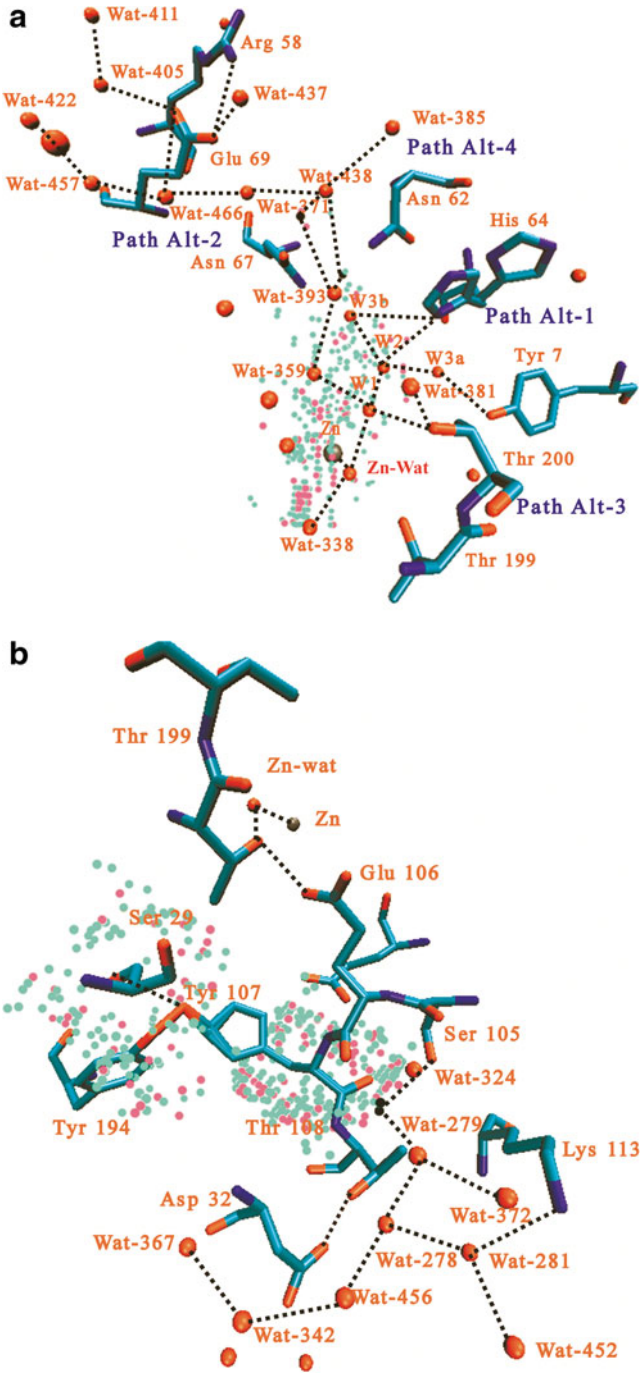

Fig. 4 Distribution of reorganized water sites from PMF study by taking center of the grid at different locations of (**a**) the active site and (**b**) the site of mutation of the mutant. The high-density water positions are designated with magenta points and low-density positions with light green points. Red spheres represent the crystal water positions in this region. The probable proton transfer pathways are shown with black dotted lines

the grid points around W1, W2 and W3b. The probability of finding such locations is much lower in the vicinity of W3a and has not been shown in Fig. 4a. None of the detected locations are found to be capable of accommodating any *additional* water molecule in the active site region.

On the contrary, these locations may be treated as disordering of one or more of the water molecules W1, W2, W3b and to a lower extent, W3a that is expected on a long timescale. Similar considerations also apply to the region between the zinc ion and the 'deep water' (Wat-338). Such disordering is expected to promote proton pathways labeled earlier as Alt-1 and 3 [6]. On the other hand, the presence of additional water molecule(s) is mostly expected in the intervening space between the residues Asn-62 and Asn-67. These sites are expected to provide a transient connection between cluster A and the solvent – exposed [29, 30] cluster containing Glu-69 and Arg-58 via the proposed pathways of Alt-2 and 4 [6].

At the site of mutation of His-107-Tyr

The results of our investigation on water occupancy near the mutation site has been shown in Fig. 4b where this region has been sampled with the center of the grid at (a) C_α atom of Tyr-107, (b) C_α atom of Ser-29 and (c) –OH atom of Tyr-194 sidechain. It is found that quite a few high and low density water sites are spread all across the region of mutation. However, most of these sites are not within hydrogen bonding distance to any of the polar amino acid sidechains, neither can they be treated as locations of disordering of crystal waters. Two low density sites are detected near Ser-105 sidechain and have been shown in Fig. 4b. It is found that a transient water molecule at any of these positions is capable of forming a hydrogen-bonded connectivity to the path Alt-3 via the residues Ser-105 and Glu-106. It can also establish a bridging connection to the hydrogen bonded cluster comprised of Asp-32, Thr-108 and Lys-113 along with several other crystal waters (Wat-278, 279, 281, 324, 342, 366, 367, 372, 412, 452, 456) [6]. Interestingly, Lys-113 and Wat-342, 372, 412, 452 form solvent exposed nodes of this cluster. Thus, a new path between the zinc-water and the protein surface is indicated that is not mediated by His-64. No analogue of this path was observed in the network analysis of the wild type enzyme starting from its crystal structure [6]. Our observations closely correspond to the probable excursions of an excess proton to this region as predicted by the multi-state empirical valence bond (MS-EVB2) simulation studies of the spatial occupancy of the center of excess charge (CEC) in the wild type enzyme [28].

Model 3

At the active site of the mutant

In this model, we investigate the effect of dynamical reorganization of the water molecules about the path connecting zinc water with His-64 by sampling equilibrated trajectories of molecular dynamics simulation of the mutant. We have selected all the simulated structures saved at a frequency of 0.5 ps from a 2 ns long equilibrated trajectory and reduced them by retaining the coordinates of all protein atoms along with 50 water molecules located nearest to the catalytic Zn^{2+} ion at the active site. Next, for each of these reduced structures, water occupancies were calculated by placing a cubic grid of 8 Å length and a grid interval of 0.25 Å choosing Zn^{2+} as the center. The sites with highest occupancies were used as the model locations of water molecules in these structures and recursive network analysis was performed on each of them. The results thus obtained corroborate closely to those obtained in model 2. Interestingly, in a significant fraction (~86 %) of the dynamically sampled structures, the outward conformer of His-64 sidechain is found to connect to the active site cluster A through one or two intervening water molecules in this region. One such typical 4-water mediated proton wire connecting the outward conformer of His-64 to zinc-water has been highlighted in Fig. 5. In addition to W1, W2 and W3b, this proton wire is found to involve one water molecule occupying a key position near the mouth of the channel bordered by Asn-62 and Trp-5. It may be noted here that this crucial water molecule permeates into the channel from the solvent. Therefore it could not be detected in our PMF studies where only the interior of the active site was sampled.

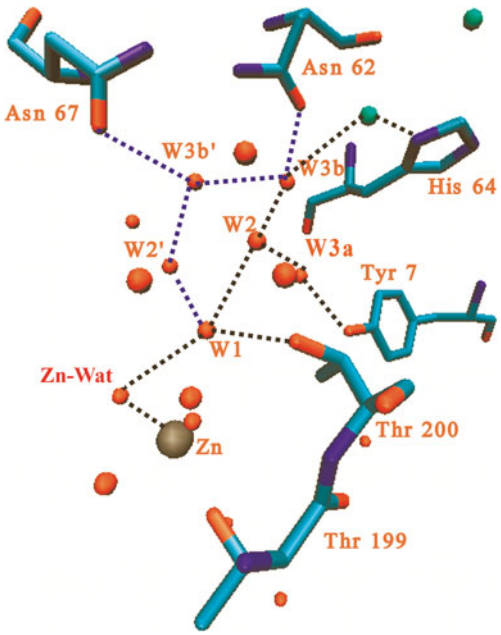

Fig. 5 Distribution of reorganized water sites from molecular dynamics simulation study by taking center of the grid at Zn^{2+} ion of the active site of the mutant. Red spheres represent the crystal water positions as well as the simulated water positions whereas green spheres represent water positions within hydrogen bonding distance of His-64 residue in this region of the last equilibrated trajectory of the simulation. The probable proton transfer pathways are shown with black dotted lines constituted by 4 water positions and that with 5 water positions are shown with blue dotted lines

Other residues such as Ser-29, Tyr-107 and Tyr-194 are found to constitute cluster C as before. However, our sampled structures did not reveal any of the nodes of cluster C to be connected directly or indirectly to the bulk solvent or to cluster A. A few water molecules forming network nodes of cluster A, on the other hand, are found to be directly exposed to the solvent in about 85% of the dynamically sampled structures. Correspondingly, dynamical reorganization of the active site clusters seem to indicate facilitation of both water mediated as well as His-64 mediated proton transfer paths.

At the site of mutation of His-107-Tyr

We have also investigated the distribution of water molecules near the site of mutation following the method as discussed above with the center of the sampling grid chosen to be at C_α atom of Tyr-107 residue. Similar to model 2, the present analysis reveals a long-lived water position near Ser-105 that might form a transient hydrogen-bonded connectivity to the path Alt-3. However, the probability of formation of the hydrogen-bonded connectivity of the mentioned water site with the O_α atom of Ser-105 residue is very low, i.e., around 0.125% with respect to the total number of dynamical structures under investigation. This might be due to the presence of this water within hydrogen bonding distance of the amide nitrogen atoms of residues Gly-104 and Ser-105 and the amide oxygen atom of Ser-105 in more than 95% and nearly 50% of all the structures sampled respectively. Any such connectivity might be expected to prevent this water molecule from participating in forming a long-lived connection to the path Alt-3. In addition, similar to model 2, we also observe the presence a solvent exposed hydrogen bonded cluster involving the residues Asp-32, Thr-108 and Lys-113. However, this cluster was not found to be connected to the path Alt-3 as in model 2, possibly due to the short length of the trajectory sampled in this study.

His-64 rotation and optimal path analysis

We next investigate the energetics of His-64 sidechain rotation that may have important contribution to the formation of a proton path into the active site. We have studied the conformational transition of His-64 from the crystallographic "outward" orientation to a target conformation that is pointing "inward" and connected via one of its sidechain N-atoms to a water molecule at the active site. Following earlier studies [6], we have retained the Asn-62 sidechain oriented away from the path of His-64 rotation. Figure 6 shows the result of optimal path analyses for a transition between the outward and inward conformers for the mutant protein. For the mutant, a series of path analyses was carried out starting from different structures constructed from models 1-3. In each case, owing to different water distributions

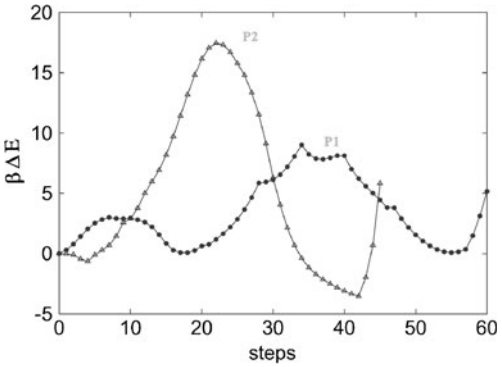

Fig. 6 The optimal paths connecting NE2 atom of outward conformation of His-64 to O atom of nearest reorganized water molecule for mutant structure following model 1 (*solid circles*) and the same path for mutant structure following model 3 (*open triangles*)

at the active site, His-64 would rotate from its outward conformation and connect to a water molecule with varying locations in the intervening region between W2 and W3b. In Fig. 6, we have shown two such representative optimal paths, P1 and P2. In each case, the optimal path is obtained from sampling of the conformational space of His-64 side chain spanned by the two dihedral angles N-C_α-C_β-C_γ (χ_1) and C_α-C_β-C_γ-$N_{\delta 1}$ (χ_2). Each dihedral angle is rotated by 5° on a periodic grid. As shown in Fig. 6, along the path P1, His-64 connects to a water molecule analogous to W2 within model 1. Along P2, His-64 connects to a water molecule corresponding to a disordered location near W3b derived from model 3. As in the wt protein [6], P1 shows two barriers that may be attributed to the unfavorable interaction of the rotating sidechain primarily with Trp-5 and its own backbone, respectively. No other side chain, polar or non-polar, is found to contribute as significantly [6]. Accordingly we have utilized different degrees of relaxation of Asn-62 and Trp-5 while estimating the optimal path within model 3. If both Asn-62 and Trp-5 are held in their crystallographic positions, one large energy barrier ($> 80\ k_BT$) is encountered along the path of rotation of His-64 sidechain to connect to W3b or its variant. Subsequent reorientations of Asn-62 lower this activation barrier to $45\ k_BT$. This further reduces to $18\ k_BT$ when both Asn-62 and Trp-5 are oriented away from the path of His-64 and the associated optimal path has been labeled as P2 in Fig. 6. It is clear from this figure that in spite of the local relaxation, a relatively large energy barrier (nearly $18\ k_BT$) still persists. This may be attributed to the clashes between His-64 sidechain and the loop region including Gly-63.

Conclusions

The main findings of the present article are summarized here. First, we have derived a series of model structures of

the mutant His-107-Tyr under the condition where this mutant is expected to be thermally stable. In the absence of any crystallographic structure, these have been utilized in carrying out an extensive analysis of water reorganization and His-64 fluctuation in the mutant His-107-Tyr to identify complete proton paths between the zinc-water and His-64. The presence or absence of the complete path is found to depend crucially on the water structure at the active site and His-64 sidechain orientation. This closely resembles the behavior of the wild type enzyme where non-trivial coupling between water reorganization and His-64 motion has already been established [6, 31]. For example, in both the wild type and the mutant, there might be a direct transfer of proton into the active site by some of the active site water molecules connecting to the protein surface. Or they may establish a transient connection to different conformers of the His-64 sidechain to complete the path. By focusing on the region of mutation, we also obtain a new proton pathway in the mutant constituted by a solvent exposed hydrogen-bonded cluster comprised of Asp-32, Thr-108, Lys-113 and several water molecules.

The results of our investigations as outlined above emphasize the competing contributions to the mechanism of proton transfer arising from water reorganization inside the active site cavity and the inward rotation of His-64 residue. The latter is found to encounter an activation barrier of about $18\ k_BT$ when critical neighboring protein segments have been allowed to relax. This value may be assumed to be an upper limit for the energy of activation as any further fluctuation in the environment of the rotating sidechain is expected to lower the activation energy further. On the other hand, the average total energy of structures having the desired 4-water mediated connection between the zinc-water and His-64 is about 67 k_BT less stable compared to the average total energy of the entire set of structures used in this study. This in turn implies a large energy cost involved in setting up the complete path only through water reorganization. It therefore, may be concluded that the optimal path for proton transfer between the zinc water and His-64 cannot be entirely attributed to either of the two main factors discussed above.

Maupin et al. studied [28] the effect of orientation of His-64 on the proton transfer event by probable excursions of an excess proton as predicted by the multi-state empirical valence bond (MS-EVB2) simulation studies of the spatial occupancy of the center of excess charge (CEC) in the wild type enzyme. By looking at the free energy barrier, they concluded that the barrier height is dominated by an Eigen cation which corresponds to water position W3b or other waters in this region when His-64 remains in its outward conformation. Our observation also supports the fact that permeation of water molecule from the bulk toward the active site near His-64 corresponding to the position of W3b will be an energy-demanding process. Moreover, the observed transient nature of the His-64 mediated path corroborates well with the earlier observation on the most probable formation of 4-5 water mediated path leading to the His-64 outward conformation with lifetimes less than 0.5 ps depending on the location of the excess proton [32].

It may be pointed out that the thermal instability of the mutant His-107-Tyr and its decrease in catalytic activity still remains an open question. In this article, we have been able to show that the mutant may be expected to have catalytic activities comparable to that of the wild type protein. However, a quantitative assessment of the connection between different degrees of disorder in the mutant structure and its reactivity is clearly beyond the scope of the present study. Since a new path is detected in the region of mutation of interest here, it may be speculated that partial denaturation of this region may even facilitate an additional proton transfer path while the others including the His-64 mediated ones may still remain operative. Work is in progress in this direction and will be reported soon.

Acknowledgements The present work has been supported in part by a grant from the Council for Scientific and Industrial Research (CSIR), India.

References

1. Håkansson K, Carlsson M, Svensson LA, Liljas A (1992) Structure of native and apo carbonic anhydrase II and structure of some of its anion-ligand complexes. J Mol Biol 227(4):1192–1204
2. Fisher Z, Hernandez Prada JA, Tu C, Duda D, Yoshioka C, An H, Govindasamy L, Silverman DN, McKenna R (2005) Structural and kinetic characterization of active-site histidine as a proton shuttle in catalysis by human carbonic anhydrase II. Biochemistry 44 (4):1097–1105. doi:10.1021/bi0480279
3. Duda D, Govindasamy L, Agbandje-McKenna M, Tu C, Silverman DN, McKenna R (2003) The refined atomic structure of carbonic anhydrase II at 1.05 A resolution: implications of chemical rescue of proton transfer. Acta Crystallogr D Biol Crystallogr 59(Pt 1):93–104
4. Silverman DN, McKenna R (2007) Solvent-mediated proton transfer in catalysis by carbonic anhydrase. Acc Chem Res 40(8):669–675. doi:10.1021/ar7000588
5. Roy A, Taraphder S (2006) Proton transfer pathways in the mutant His-64-Ala of human carbonic anhydrase II. Biopolymers 82 (6):623–630. doi:10.1002/Bip.20516
6. Roy A, Taraphder S (2007) Identification of proton-transfer pathways in human carbonic anhydrase II. J Phys Chem B 111 (35):10563–10576. doi:10.1021/Jp073499t
7. Steiner H, Jonsson BH, Lindskog S (1975) The catalytic mechanism of carbonic anhydrase. Hydrogen-isotope effects on the kinetic parameters of the human C isoenzyme. Eur J Biochem 59 (1):253–259
8. Silverman DN (2000) Marcus rate theory applied to enzymatic proton transfer. Biochim Biophys Acta 1458(1):88–103
9. Silverman DN, Lindskog S (1988) Acc Chem Res 21:30-36
10. Forsman C, Behravan G, Jonsson BH, Liang ZW, Lindskog S, Ren XL, Sandstrom J, Wallgren K (1988) Histidine 64 is not required for high CO2 hydration activity of human carbonic anhydrase II. FEBS Lett 229(2):360–362

11. Tu CK, Silverman DN, Forsman C, Jonsson BH, Lindskog S (1989) Role of histidine 64 in the catalytic mechanism of human carbonic anhydrase II studied with a site-specific mutant. Biochemistry 28(19):7913–7918
12. Roy A, Taraphder S (2008) A theoretical study on the detection of proton transfer pathways in some mutants of human carbonic anhydrase II. J Phys Chem B 112(43):13597–13607. doi:10.1021/Jp0757309
13. Tashian RE (1989) The carbonic anhydrases: widening perspectives on their evolution, expression and function. Bioessays 10 (6):186–192. doi:10.1002/bies.950100603
14. Eriksson AE, Jones TA, Liljas A (1988) Refined structure of human carbonic anhydrase II at 2.0 A resolution. Proteins 4 (4):274–282. doi:10.1002/prot.340040406
15. Sly WS, Hewett-Emmett D, Whyte MP, Yu YS, Tashian RE (1983) Carbonic anhydrase II deficiency identified as the primary defect in the autosomal recessive syndrome of osteopetrosis with renal tubular acidosis and cerebral calcification. Proc Natl Acad Sci USA 80(9):2752–2756
16. Tu C, Couton JM, Van Heeke G, Richards NG, Silverman DN (1993) Kinetic analysis of a mutant (His107–>Tyr) responsible for human carbonic anhydrase II deficiency syndrome. J Biol Chem 268(7):4775–4779
17. Venta PJ, Welty RJ, Johnson TM, Sly WS, Tashian RE (1991) Carbonic anhydrase II deficiency syndrome in a Belgian family is caused by a point mutation at an invariant histidine residue (107 His—Tyr): complete structure of the normal human CA II gene. Am J Hum Genet 49(5):1082–1090
18. Almstedt K, Lundqvist M, Carlsson J, Karlsson M, Persson B, Jonsson BH, Carlsson U, Hammarstrom P (2004) Unfolding a folding disease: folding, misfolding and aggregation of the marble brain syndrome-associated mutant H107Y of human carbonic anhydrase II. J Mol Biol 342:619–633. doi:10.1016/j.jmb.2004.07.024
19. Garcia AE, Hummer G, Soumpasis DM (1997) Hydration of an alpha-helical peptide: comparison of theory and molecular dynamics simulation. Proteins 27(4):471–480
20. Phillips JC, Braun R, Wang W, Gumbart J, Tajkhorshid E, Villa E, Chipot C, Skeel RD, Kale L, Schulten K (2005) Scalable molecular dynamics with NAMD. J Comput Chem 26(16):1781–1802. doi:10.1002/Jcc.20289
21. Humphrey W, Dalke A, Schulten K (1996) VMD: visual molecular dynamics. J Mol Graph Model 14(1):33–38
22. MacKerell AD, Bashford D, Bellott M, Dunbrack RL, Evanseck JD, Field MJ, Fischer S, Gao J, Guo H, Ha S, Joseph-McCarthy D, Kuchnir L, Kuczera K, Lau FTK, Mattos C, Michnick S, Ngo T, Nguyen DT, Prodhom B, Reiher WE, Roux B, Schlenkrich M, Smith JC, Stote R, Straub J, Watanabe M, Wiorkiewicz-Kuczera J, Yin D, Karplus M (1998) All-atom empirical potential for molecular modeling and dynamics studies of proteins. J Phys Chem B 102(18):3586–3616
23. Feller S, Zhang Y, Pastor R, Brooks B (1995) J Chem Phys 103:4613
24. Taraphder S, Hummer G (2003) Protein side-chain motion and hydration in proton-transfer pathways. Results for cytochrome p450cam. J Am Chem Soc 125(13):3931–3940. doi:10.1021/ja016860c
25. Dijkstra EW (1959) Numer Math 1:269-271
26. Taraphder S, Hummer G (2003) Dynamic proton transfer pathways in proteins: role of sidechain conformational fluctuations. Physica A 318(1–2):293–301
27. Fisher SZ, Maupin CM, Budayova-Spano M, Govindasamy L, Tu C, Agbandje-McKenna M, Silverman DN, Voth GA, McKenna R (2007) Atomic crystal and molecular dynamics simulation structures of human carbonic anhydrase II: insights into the proton transfer mechanism. Biochemistry 46(11):2930–2937. doi:10.1021/bi062066y
28. Maupin CM, McKenna R, Silverman DN, Voth GA (2009) Elucidation of the proton transport mechanism in human carbonic anhydrase II. J Am Chem Soc 131(22):7598–7608. doi:10.1021/ja8091938
29. Lee B, Richards FM (1971) J Mol Biol 55:379
30. Hubbard SJ, Thorton JM (1993). NACCESS, Computer program; Department of Biochemistry and Molecular Biology, University College London
31. Roy A, Taraphder S (2010) Role of protein motions on proton transfer pathways in human carbonic anhydrase II. BBA Proteins Proteomics 1804(2):352–361. doi:10.1016/j.bbapap.2009.09.004
32. Maupin CM, Voth GA (2010) Proton transport in carbonic anhydrase: insights from molecular simulation. Biochim Biophys Acta 1804(2):332–341